

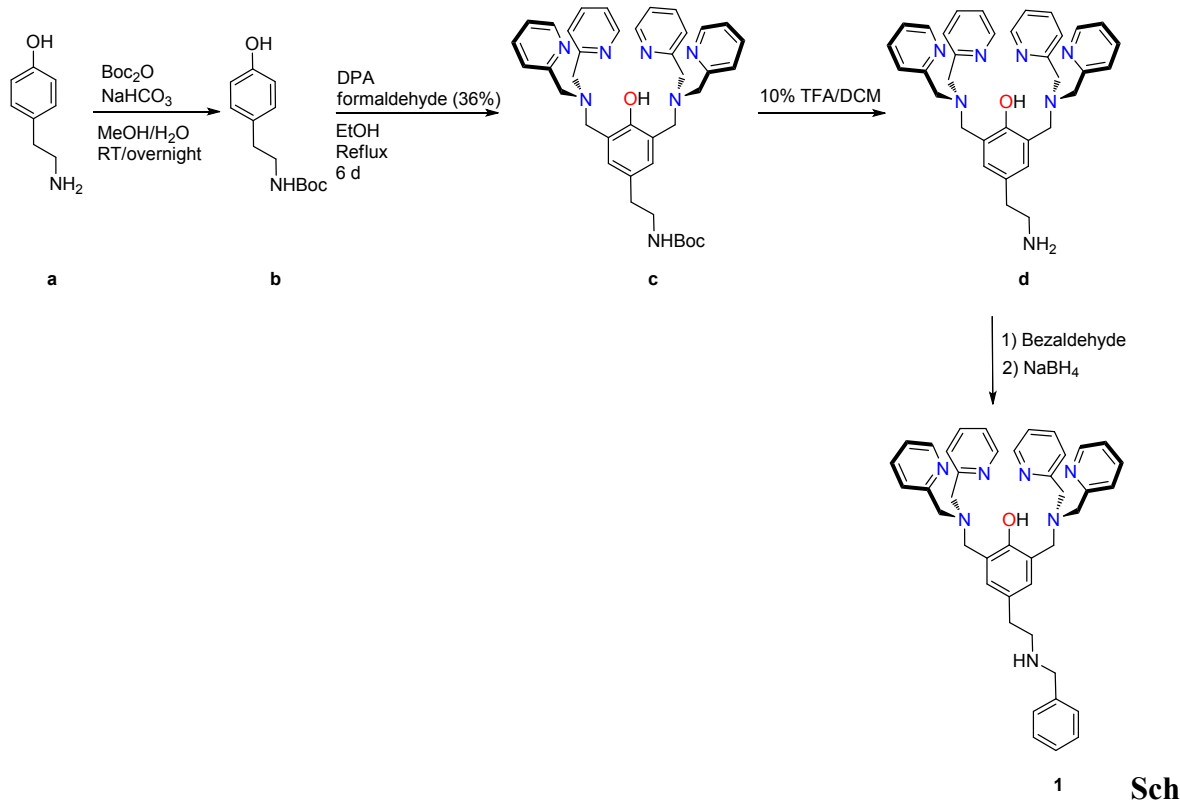
Supporting information

Molecular recognition of bisphosphonate-based drugs by di-zinc receptors in aqueous solution and on gold nanoparticles

Aaron Torres-Huerta,¹ Tiffany G. Chan,¹ Andrew J.P. White, Ramon Vilar^{*1}.

¹*Department of Chemistry, Imperial College London, White City Campus, London W12*

OBZ (UK)



eme S1: Synthesis route of the compound **1**.

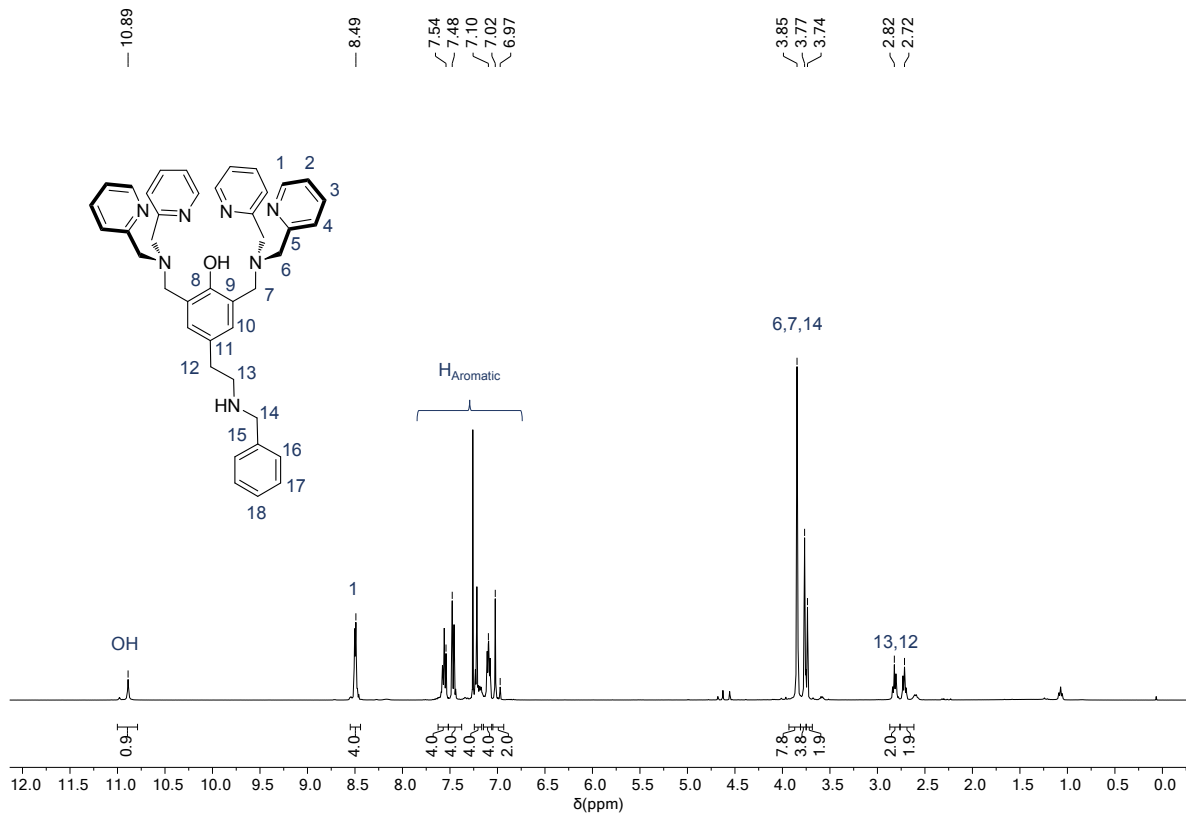


Figure S1: ^1H NMR spectrum of compound 1.

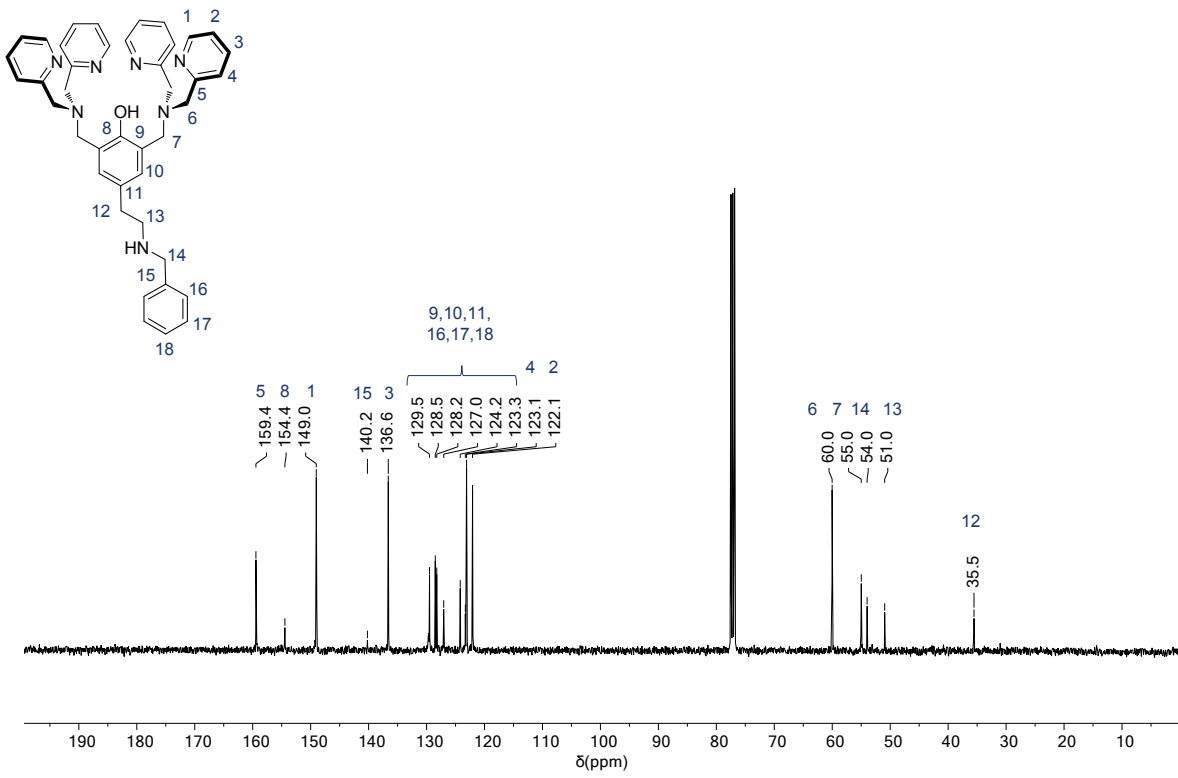


Figure S2: ^{13}C NMR spectrum of compound 1.

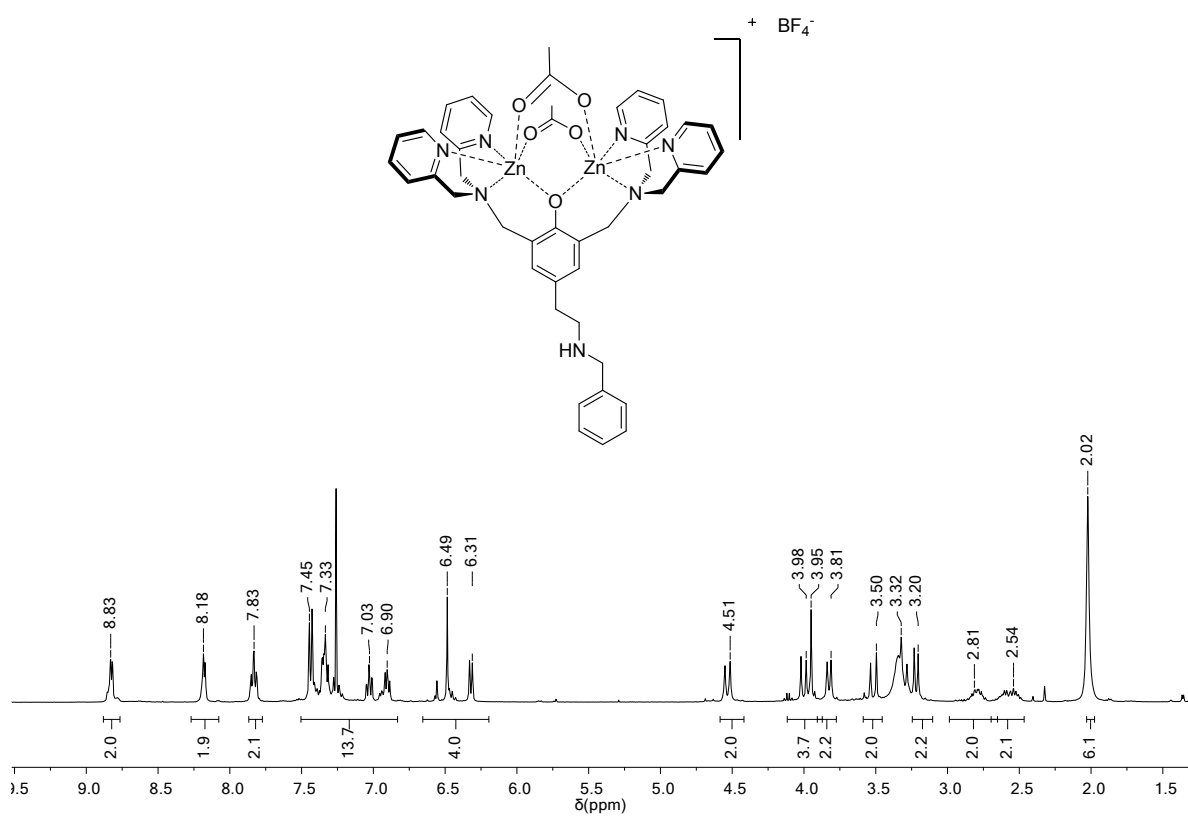


Figure S3: ^1H NMR spectrum of compound 2.

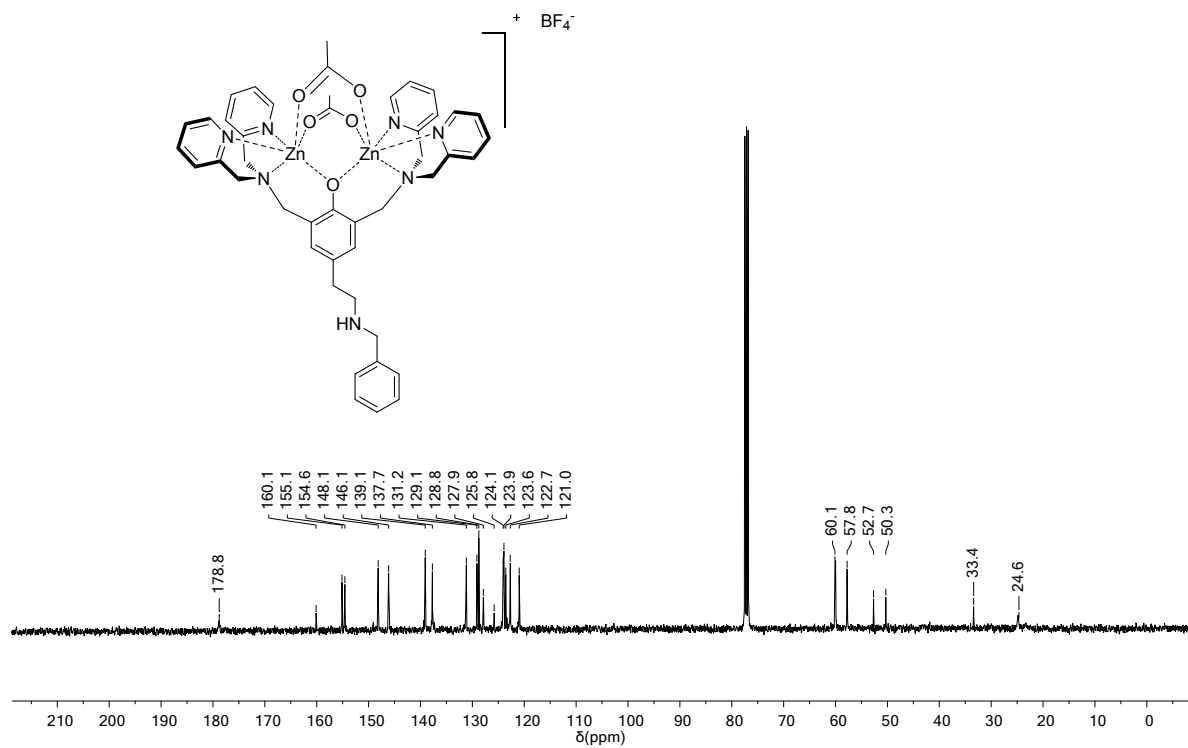


Figure S4: ^{13}C NMR spectrum of compound **2**.

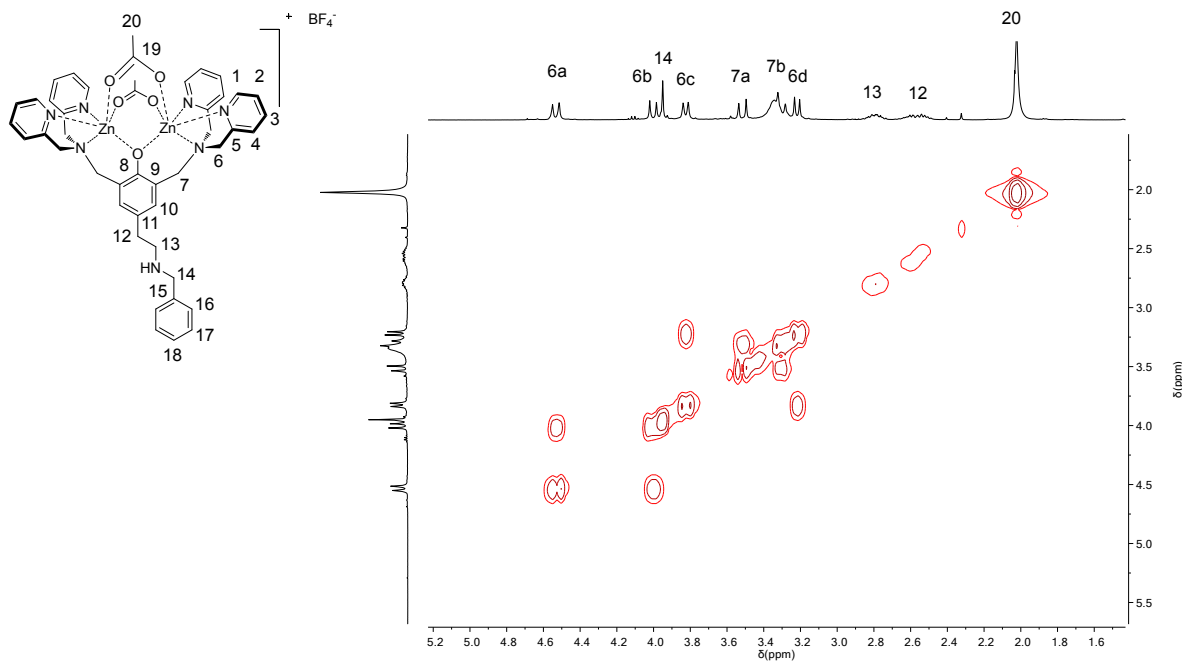


Figure S5: COSY NMR spectrum of compound 2 (aliphatic region).

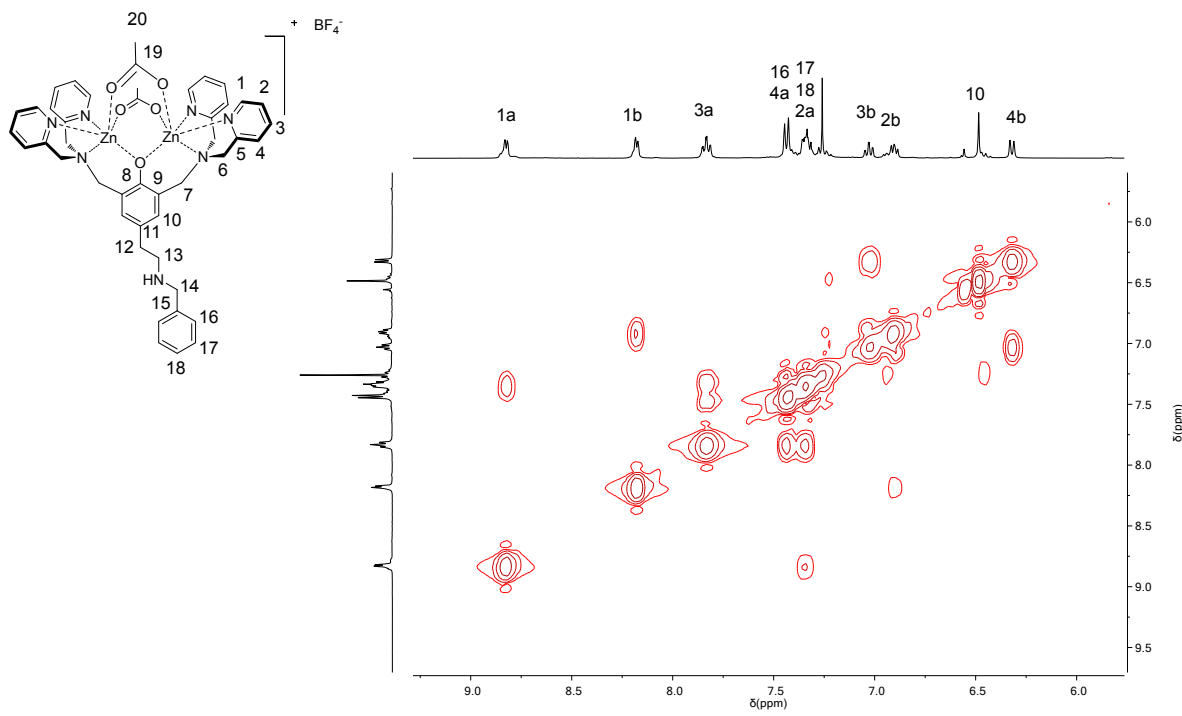


Figure S6: COSY NMR spectrum of compound 2 (aromatic region).

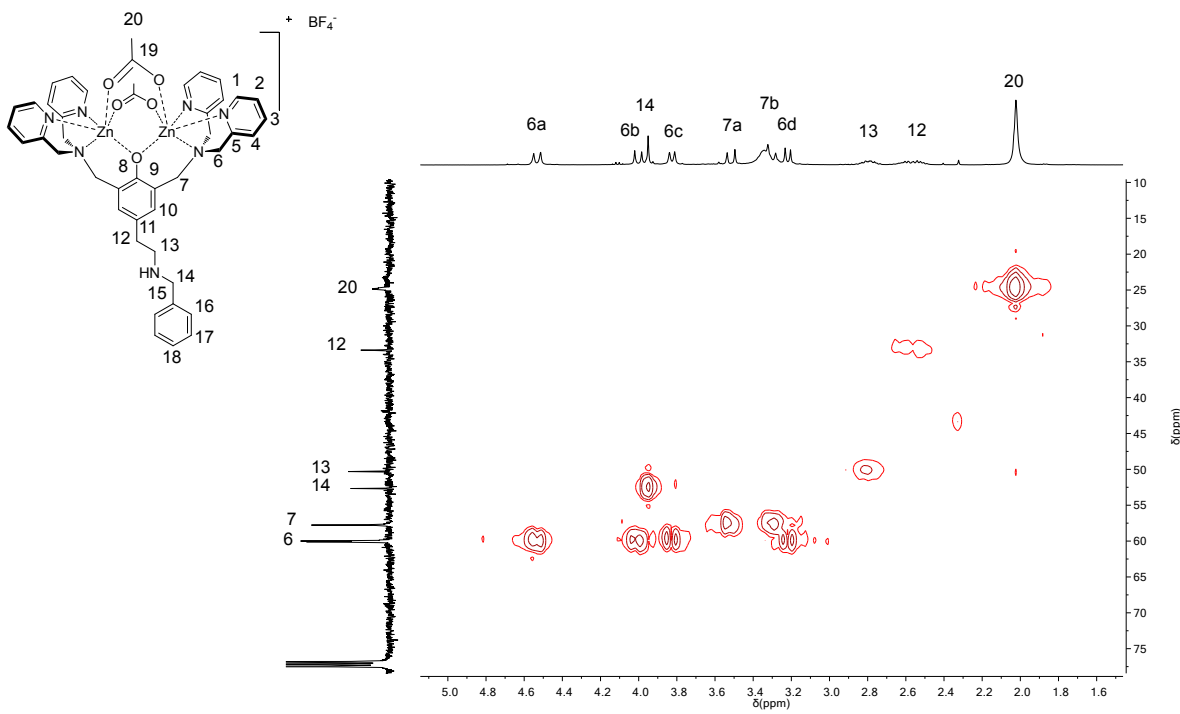


Figure S7: HSQC NMR spectrum of compound 2 (aliphatic region).

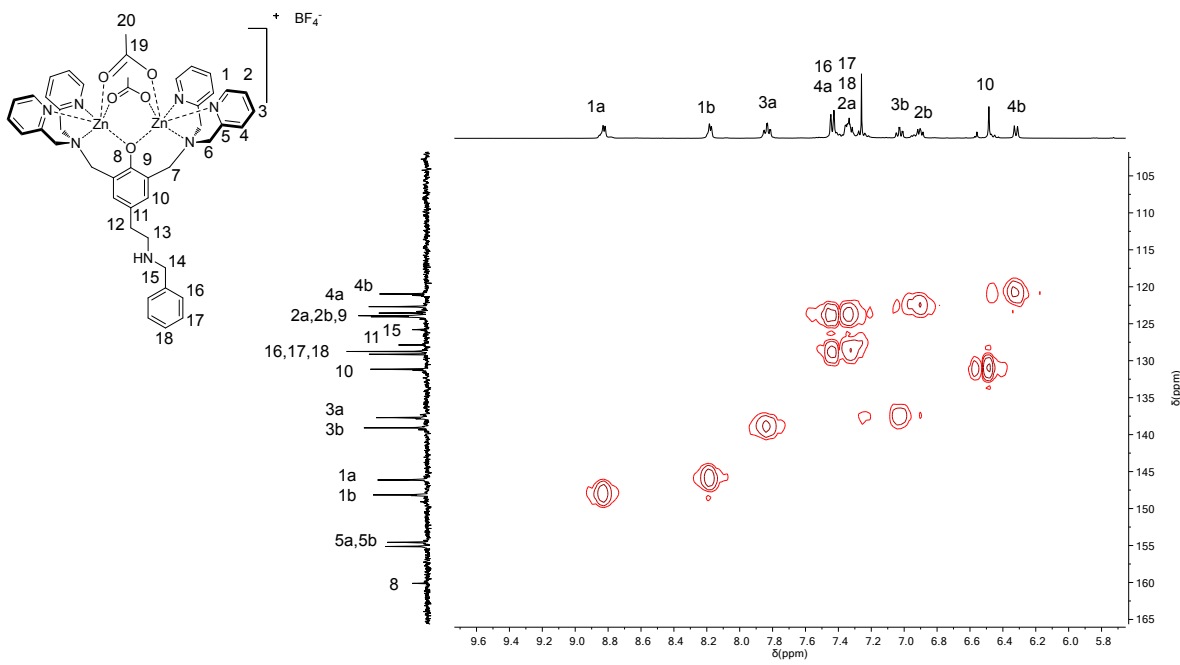


Figure S8: HSQC NMR spectrum of compound 2 (aromatic region).

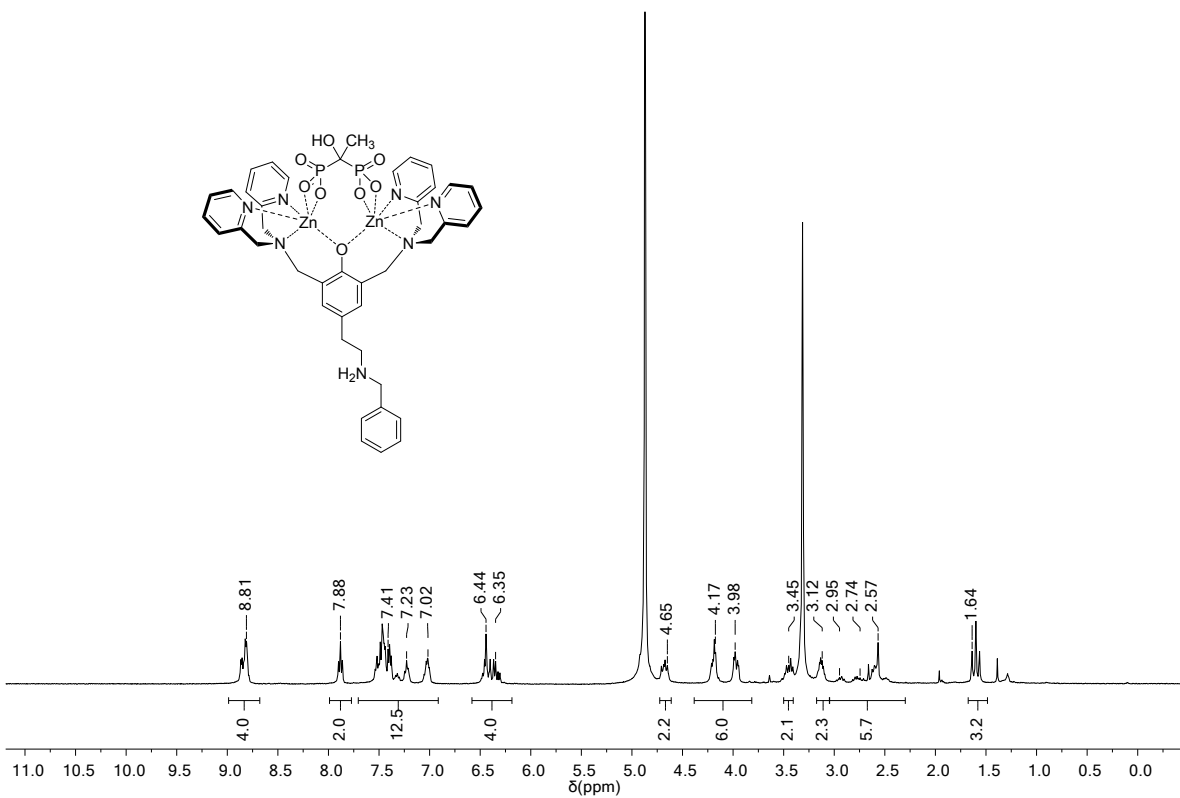


Figure S9: ¹H NMR spectrum of compound 3.

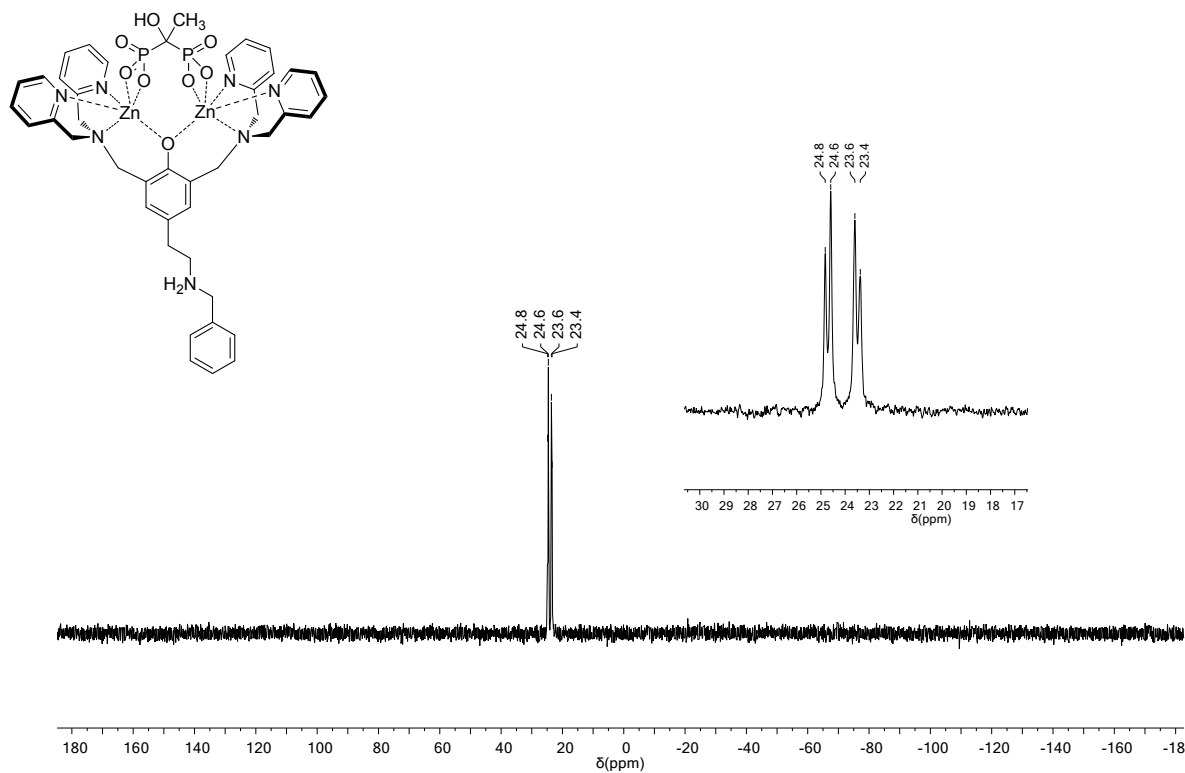


Figure S10: ³¹P NMR spectrum of compound 3.

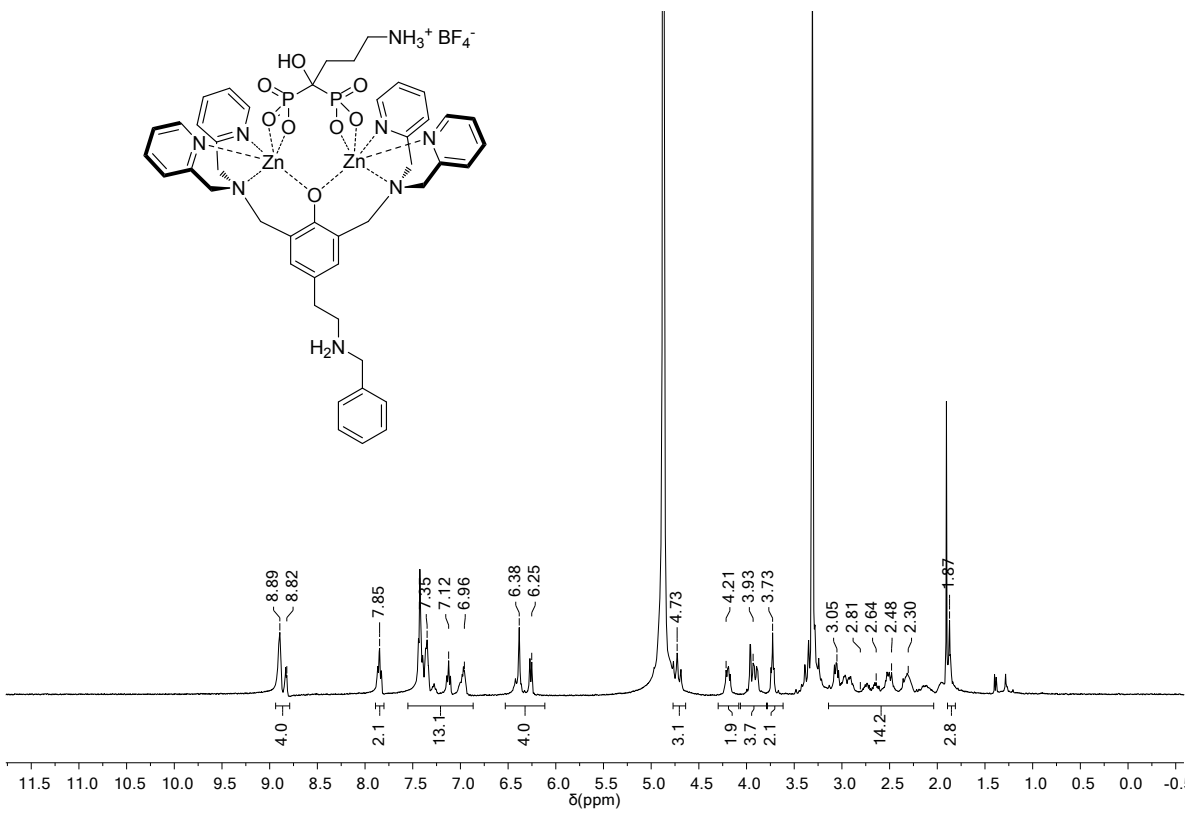


Figure S11: ¹H NMR spectrum of compound 4.

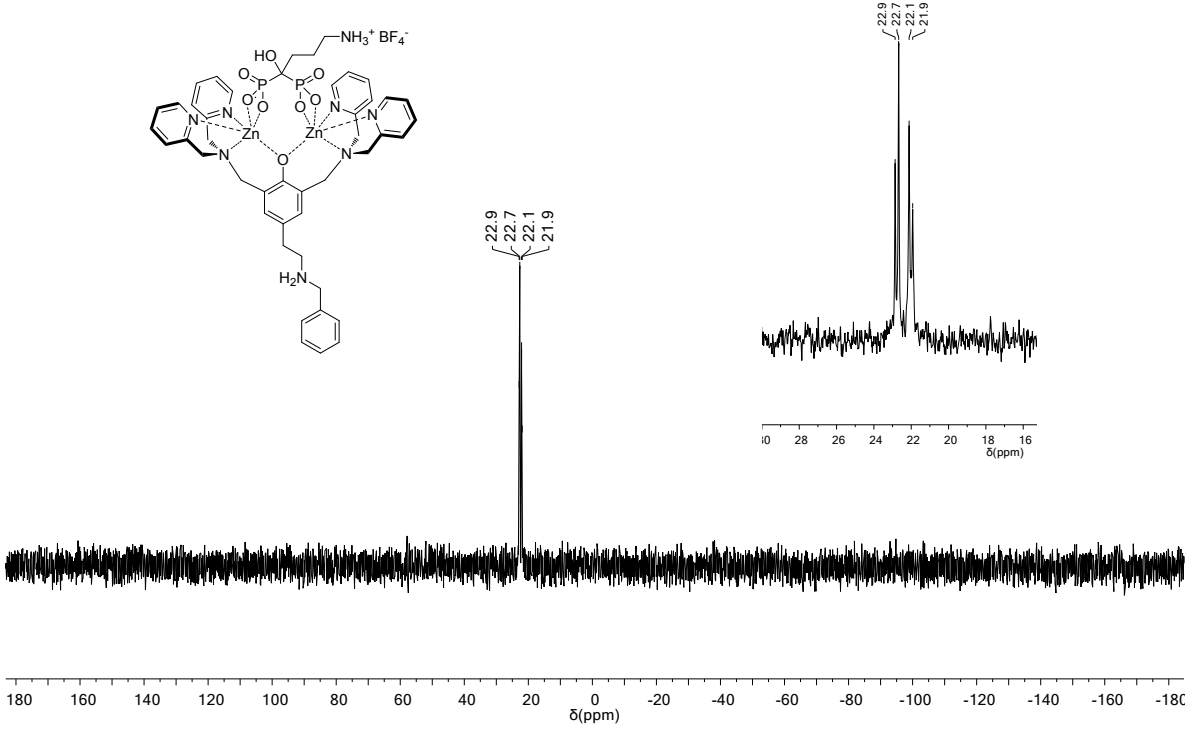


Figure S12: ³¹P NMR spectrum of compound 4.

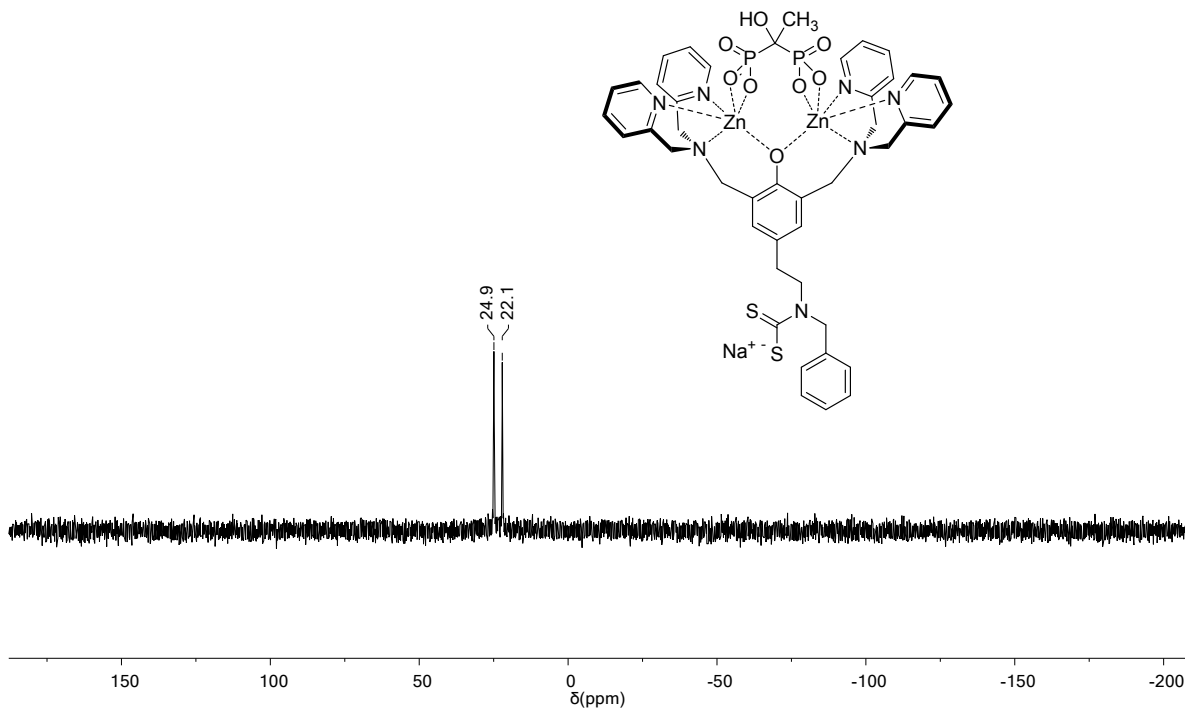


Figure S13: ^{31}P NMR spectrum of compound 6.

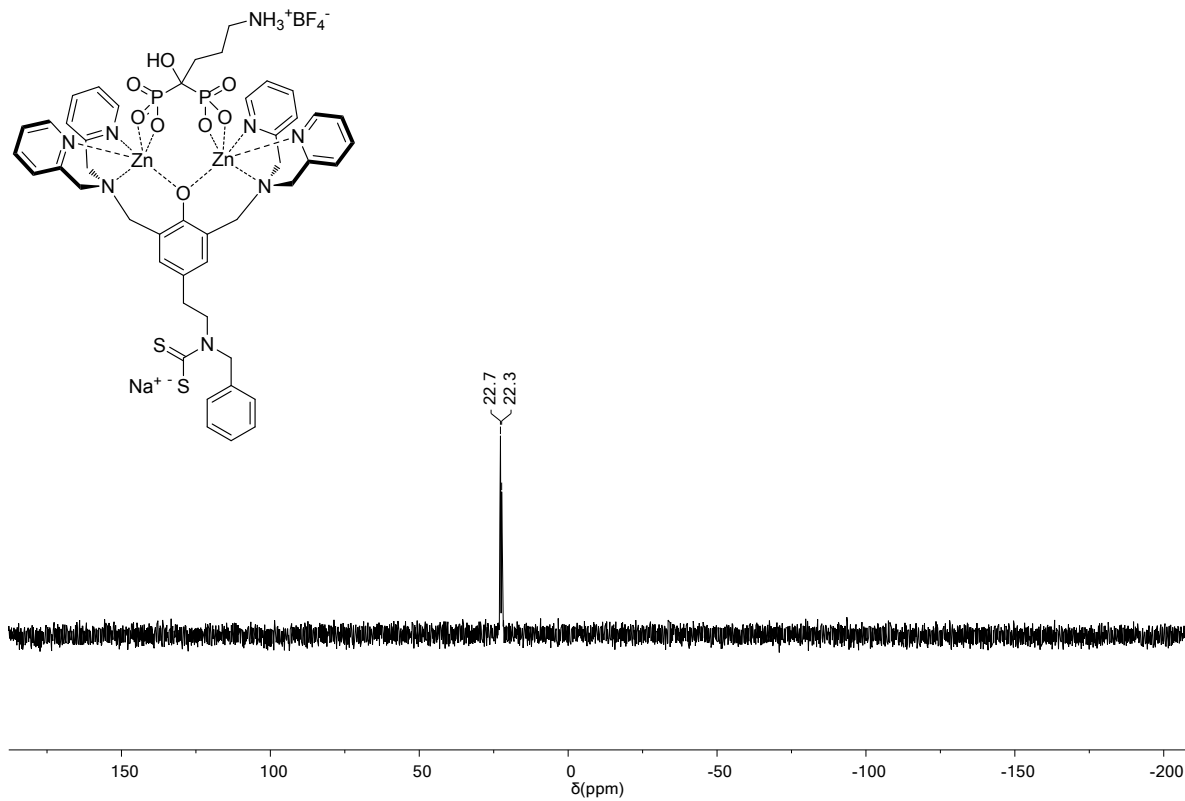


Figure S14: ^{31}P NMR spectrum of compound 7.

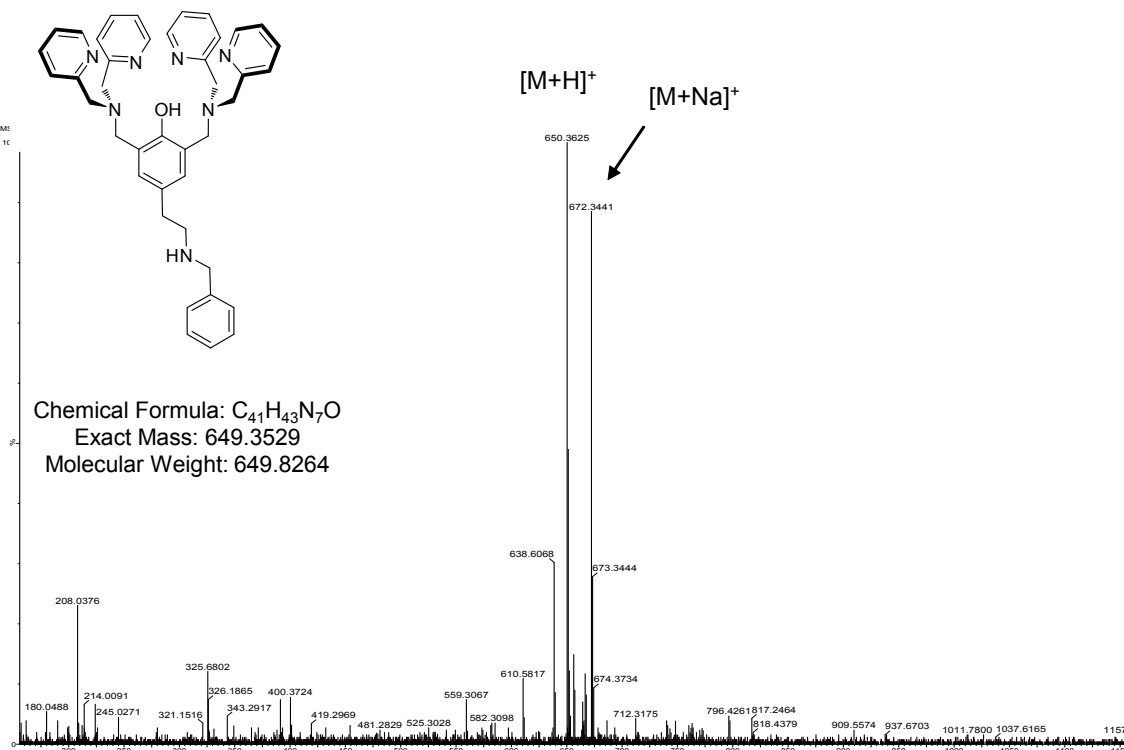


Figure S15: Mass spectrum of compound 1.

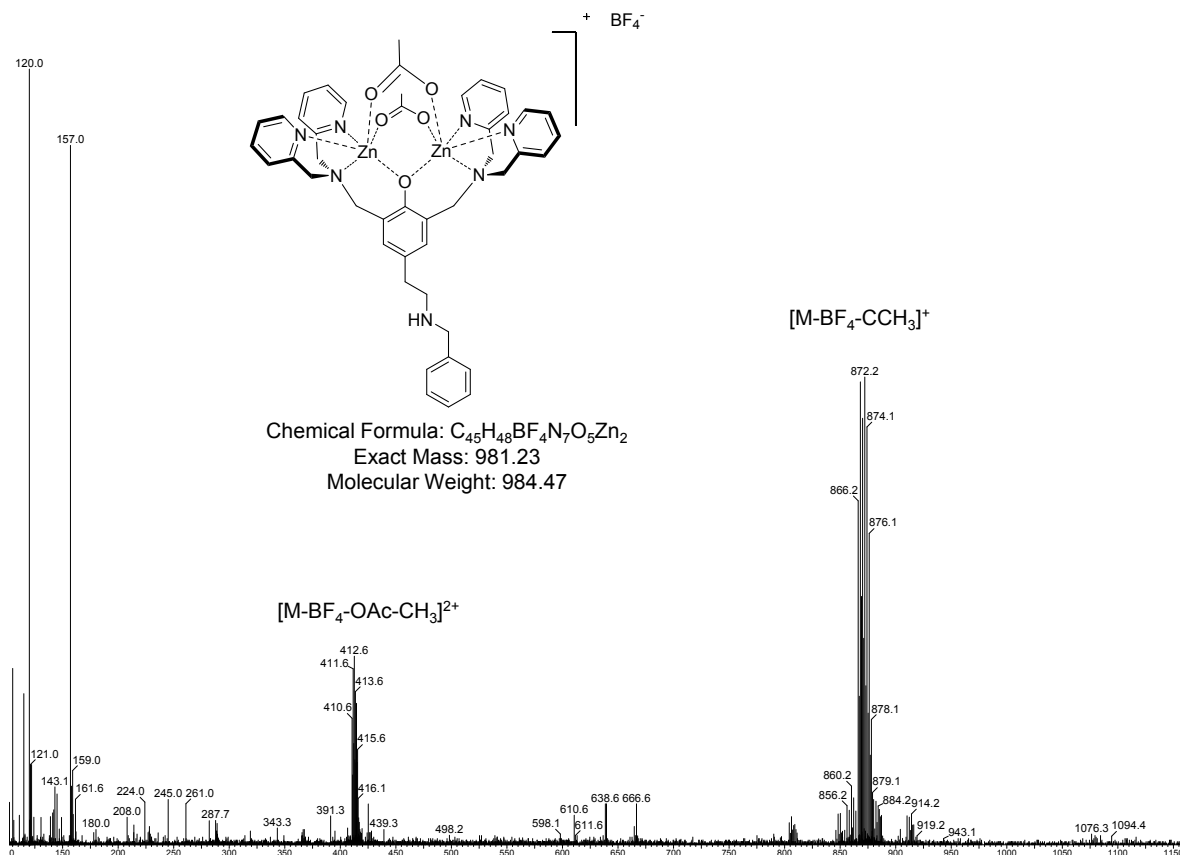


Figure S16: Mass spectrum of compound 2.

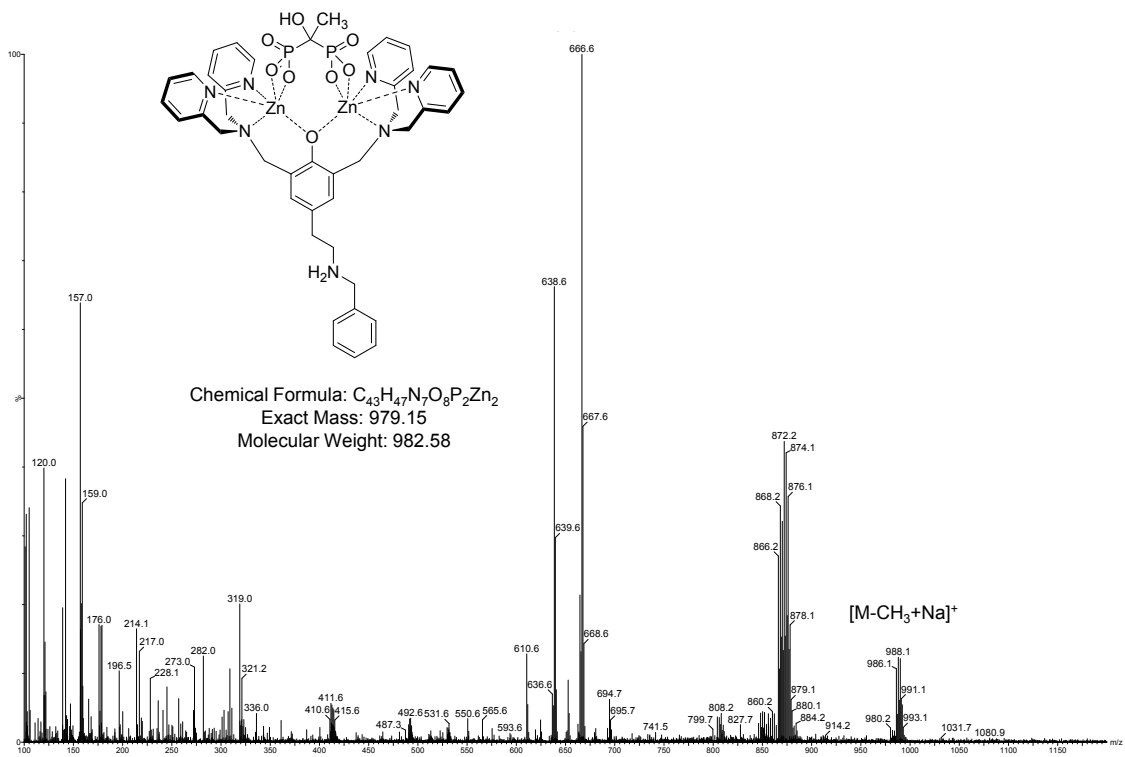


Figure S17: Mass spectrum of compound 3.

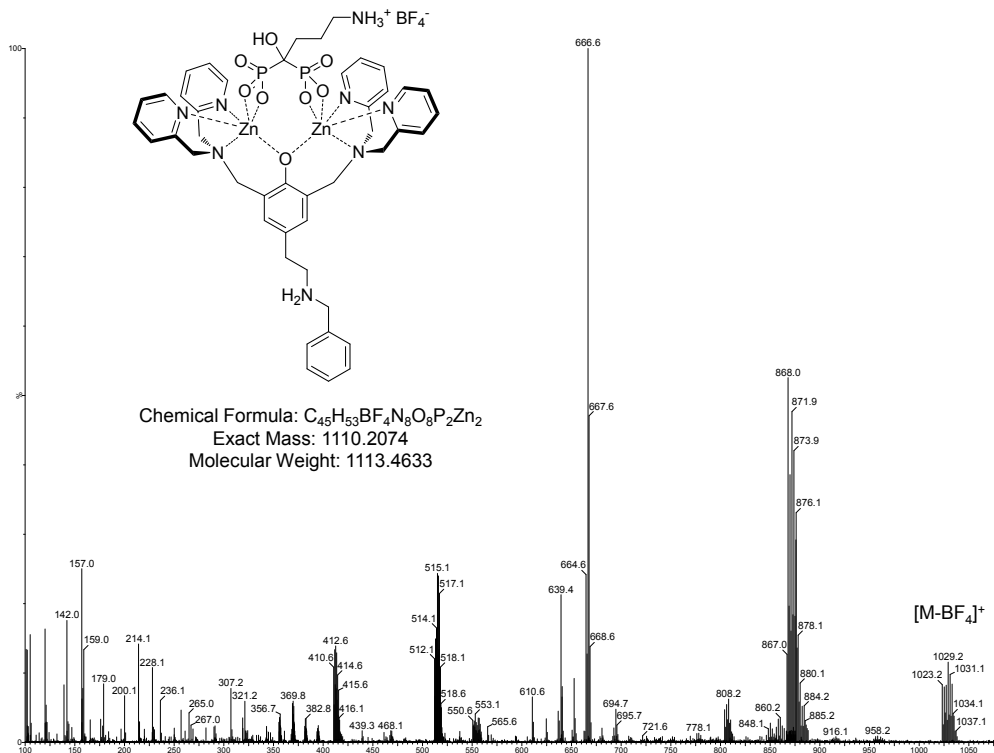


Figure S18: Mass spectrum of compound 4.

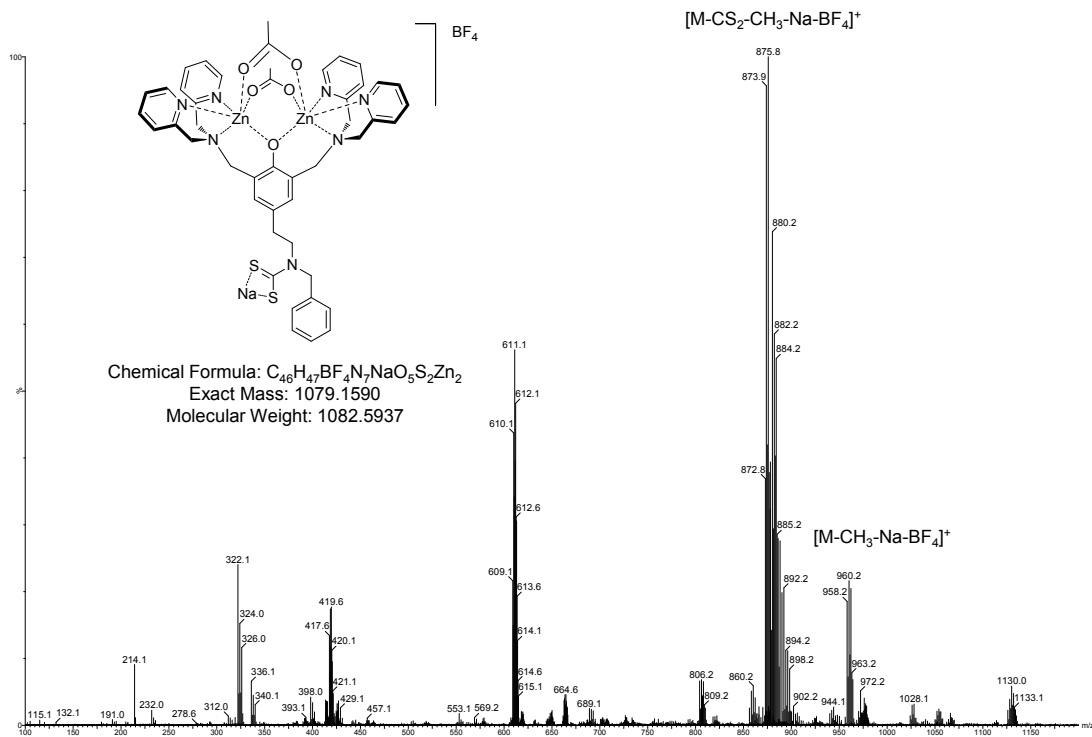


Figure S19: Mass spectrum of compound 5.

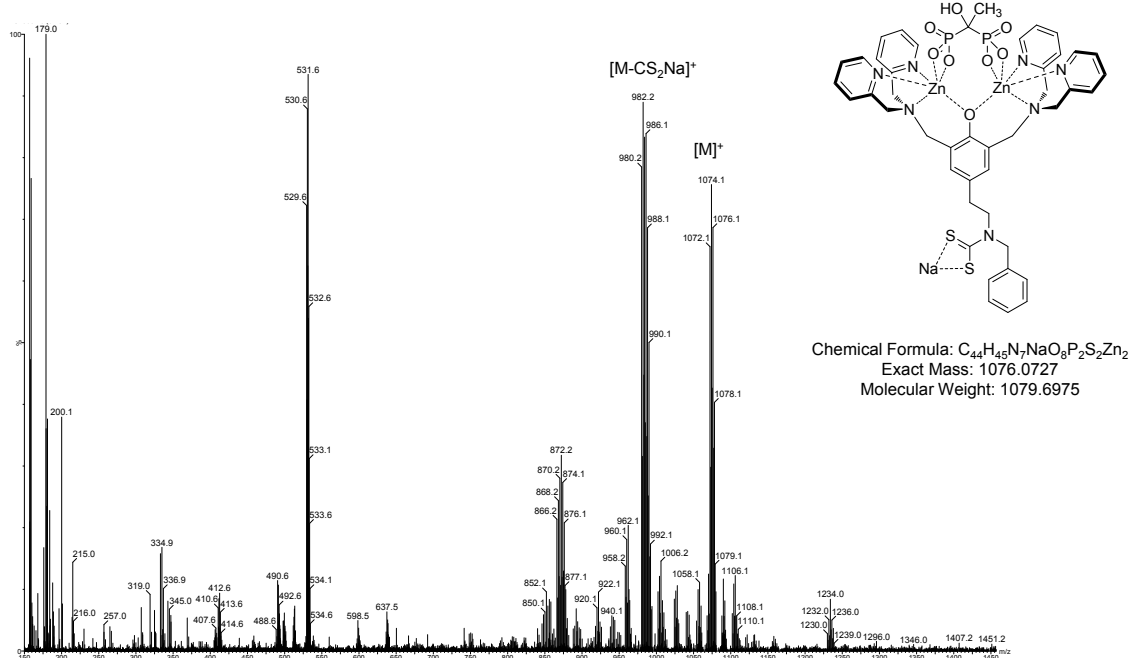


Figure S20: Mass spectrum of compound 6.

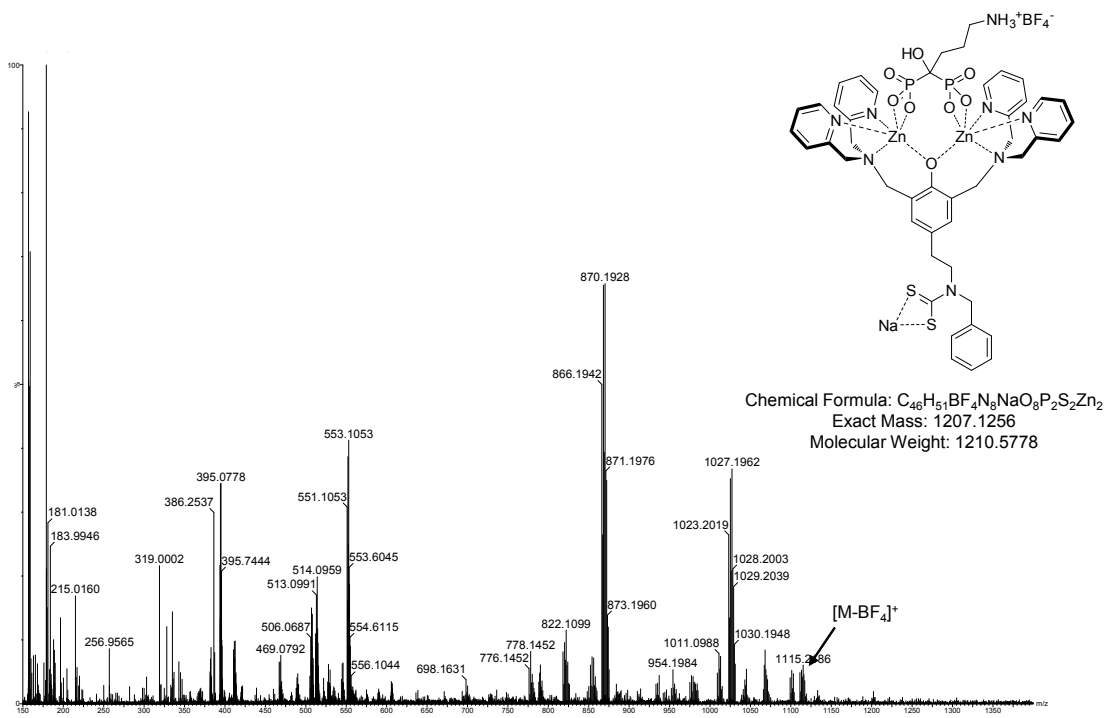


Figure S21: Mass spectrum of compound 7.

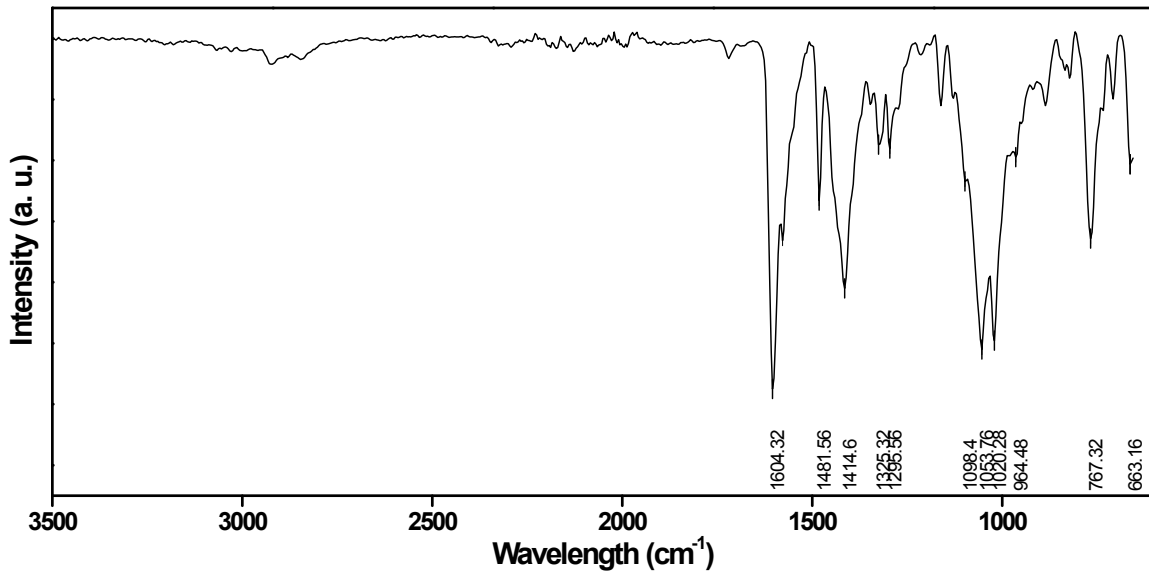


Figure S22: FT-IR (ATR) spectrum of compound 2.

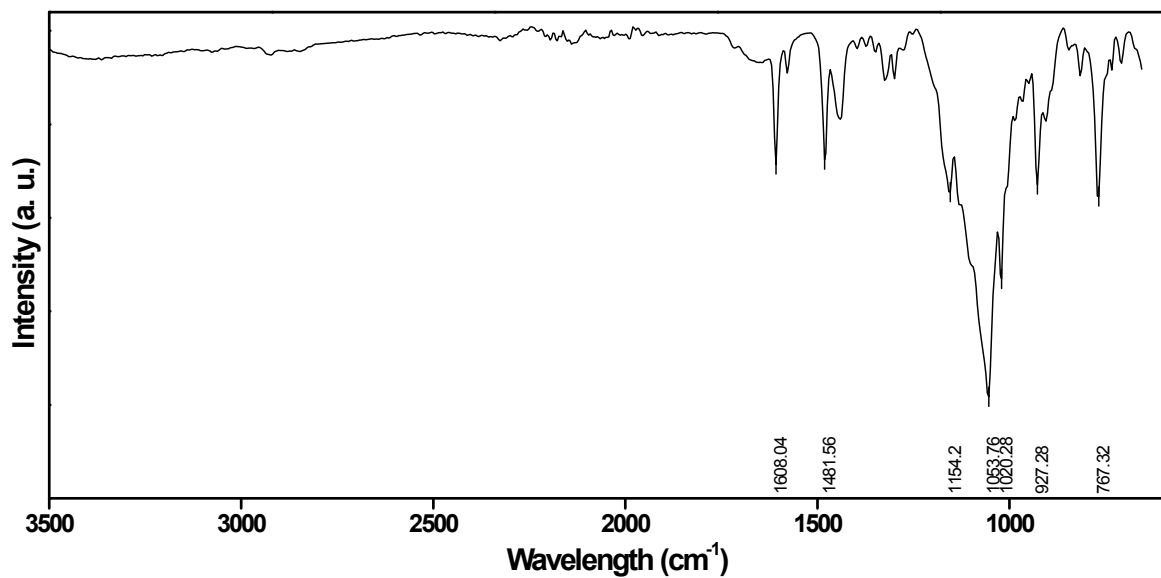


Figure S23: FT-IR (ATR) spectrum of compound 3.

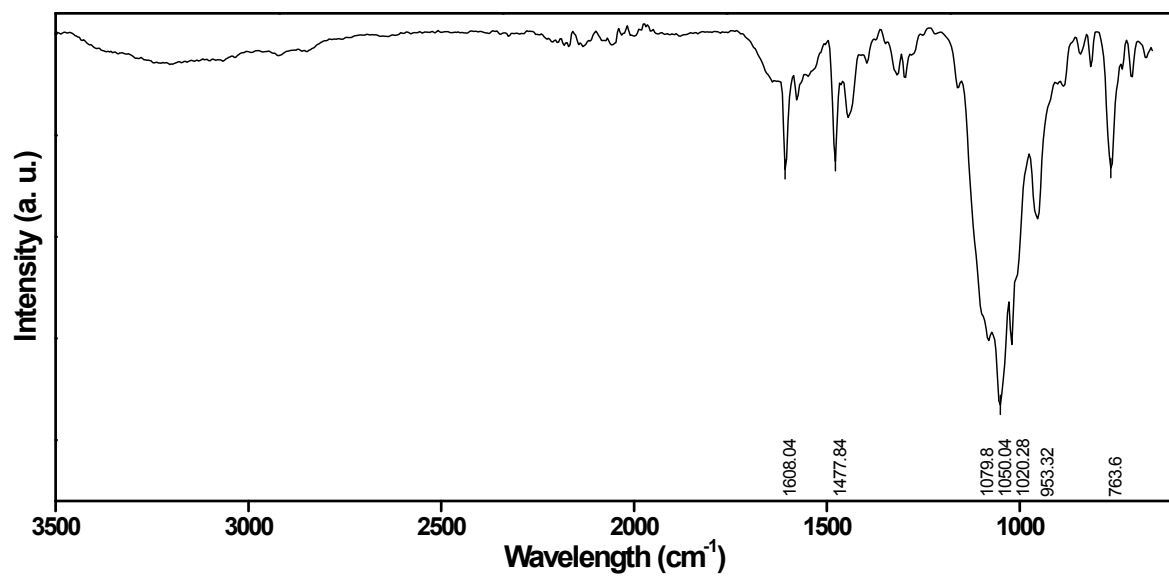


Figure S24: FT-IR (ATR) spectrum of compound 4.

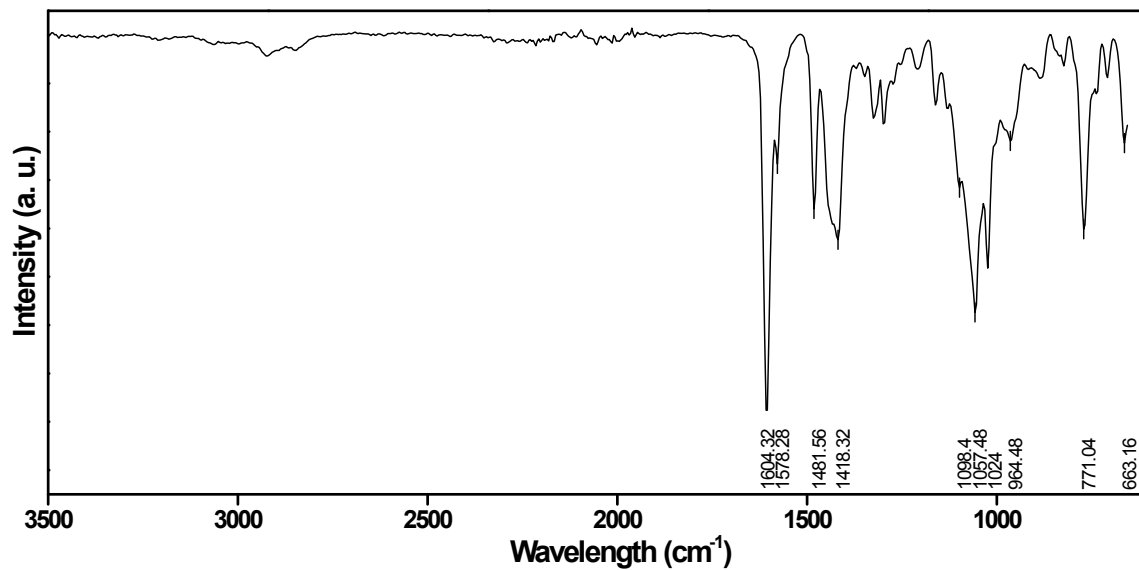


Figure S25: FT-IR (ATR) spectrum of compound 5.

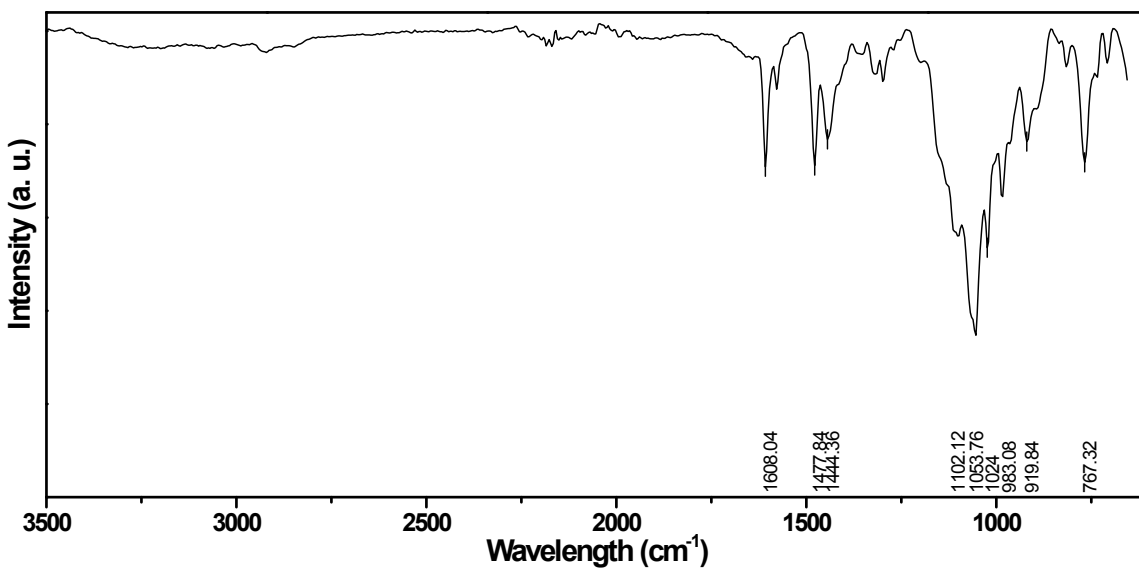


Figure S26: FT-IR (ATR) spectrum of compound 6.

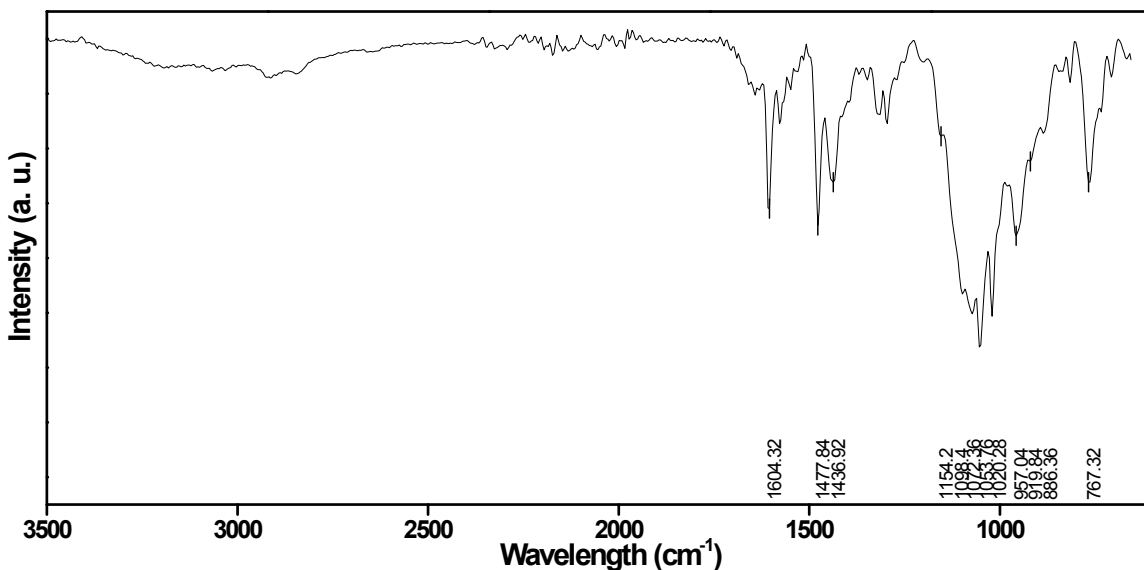


Figure S27: FT-IR (ATR) spectrum of compound 7.

The X-ray crystal structure of 3

The included solvent in the structure of **3** was found to be highly disordered, and the best approach to handling this diffuse electron density was found to be the SQUEEZE routine of PLATON.¹ This suggested a total of 250 electrons per unit cell, equivalent to 125 electrons per asymmetric unit. Before the use of SQUEEZE the solvent most resembled numerous water molecules (H_2O , 10 electrons), and 12.5 water molecules corresponds to 125 electrons, so this was used as the solvent present. As a result, the atom list for the asymmetric unit is low by $12.5(\text{H}_2\text{O}) = \text{H}_{25}\text{O}_{12.5}$ (and that for the unit cell low by $\text{H}_{50}\text{O}_{25}$) compared to what is actually presumed to be present.

The hydrogen atoms of the N42-based NH_2 group were located from ΔF maps and refined freely subject to an N–H distance constraint of 0.90 Å. The presumed hydrogen atom of the O59-based OH group, however, could not be reliably located and so the atom list for the asymmetric unit is low by H_1 , and that for the unit cell low by H_2 , making the discrepancy $\text{H}_{52}\text{O}_{25}$ in total.

The X-ray crystal structure of 4

Part of the included solvent in the structure of **4** was found to be highly disordered, and the best approach to handling this diffuse electron density was found to be the SQUEEZE routine of PLATON.¹ This suggested a total of 55 electrons per unit cell, equivalent to 27.5 electrons per asymmetric unit. Before the use of SQUEEZE the solvent most resembled methanol (CH_4O , 18 electrons), and 1.5 methanol molecules corresponds to 27 electrons, so this was used as the solvent present. As a result, the atom list for the asymmetric unit is low by $1.5(\text{CH}_4\text{O}) = \text{C}_{1.5}\text{H}_6\text{O}_{1.5}$ (and that for the unit cell low by $\text{C}_3\text{H}_{12}\text{O}_3$) compared to what is actually presumed to be present.

The hydrogen atoms of the N42-based NH_2 group were located from ΔF maps and refined freely subject to an N–H distance constraint of 0.90 Å. The presumed hydrogen atoms of the O59-based OH group, the N63-based NH_3^+ -group, and the O91- to O98-based water molecules however, could not be reliably located and so the atom list for the asymmetric unit is low by H_{20} , and that for the unit cell low by H_{40} , making the discrepancy $\text{C}_3\text{H}_{52}\text{O}_3$ in total.

The B70-based tetrafluoroborate anion was found to be disordered, and two orientations were identified of *ca.* 84 and 16% occupancy with the central boron and one (F71) of the fluorine atoms being common to both. The geometries of both orientations were optimised, the thermal parameters of adjacent atoms were restrained to be similar, and only the non-hydrogen atoms of the major occupancy orientation were refined anisotropically (those of the minor occupancy orientation were refined isotropically).

The C80-based included toluene solvent molecule was found to be disordered across a centre of symmetry, and two unique orientations were identified of *ca.* 33 and 17% occupancy (with two further orientations of the same occupancies being generated by operation of the inversion centre). The geometries of both unique orientations were optimised, the thermal parameters of adjacent atoms were restrained to be similar, and all of the atoms of both orientations were refined isotropically.

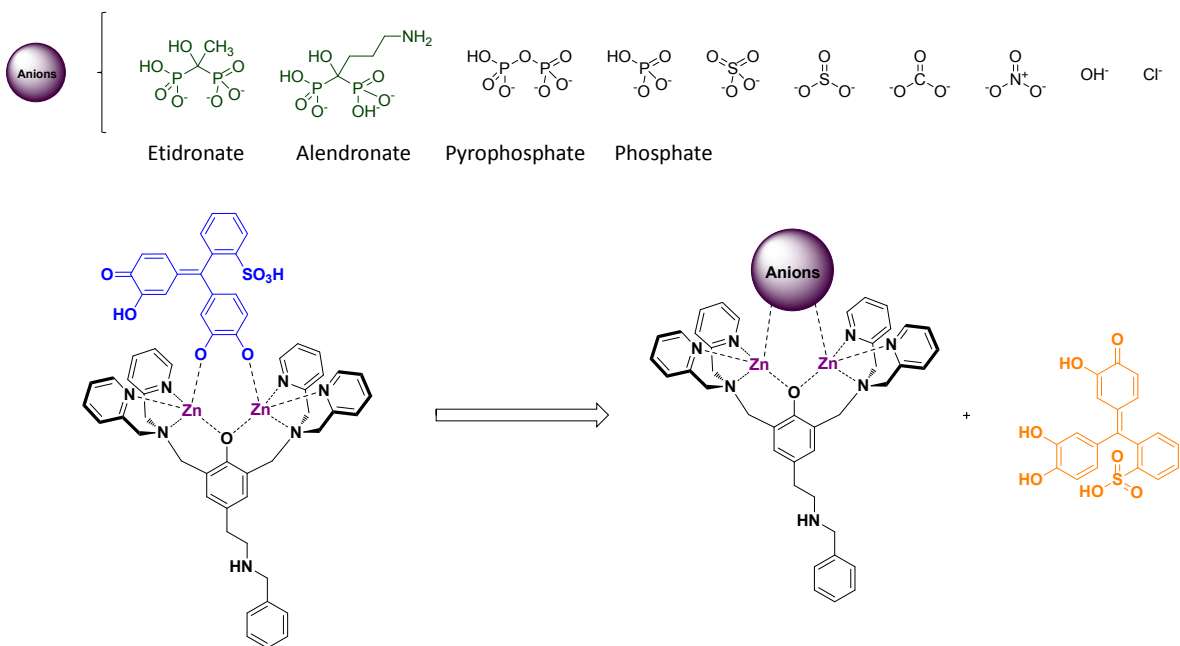
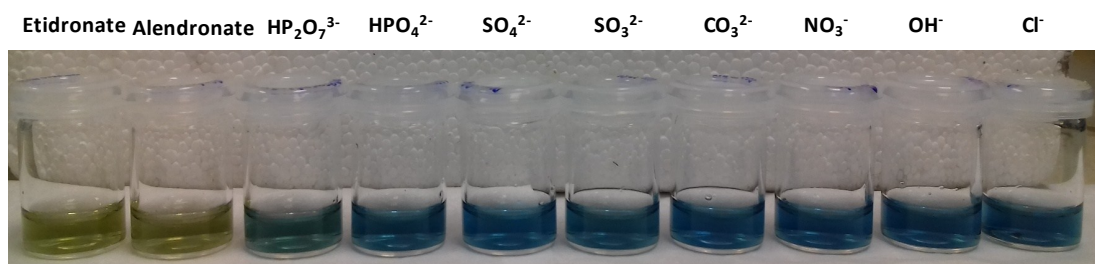


Figure S28: Indicator displacement assay for etidronate and alendronate bisphosphonate drugs and regular inorganic anions.

a)



b)

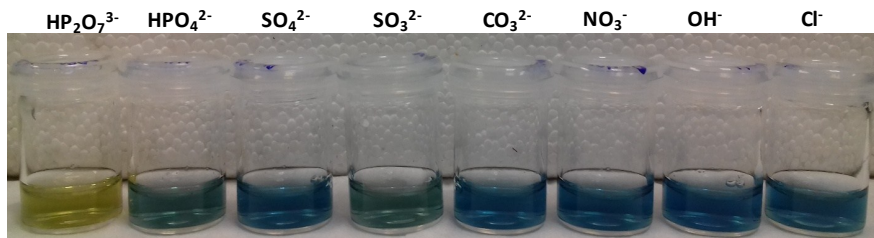


Figure S29: Colorimetric response of **2·PV** in 10 mM HEPES solution at pH 7.4 at room temperature. a) With 1 eq of etidronate and alendronate as well as with the regular inorganic anions. b) With 10 eq. of regular inorganic anions.

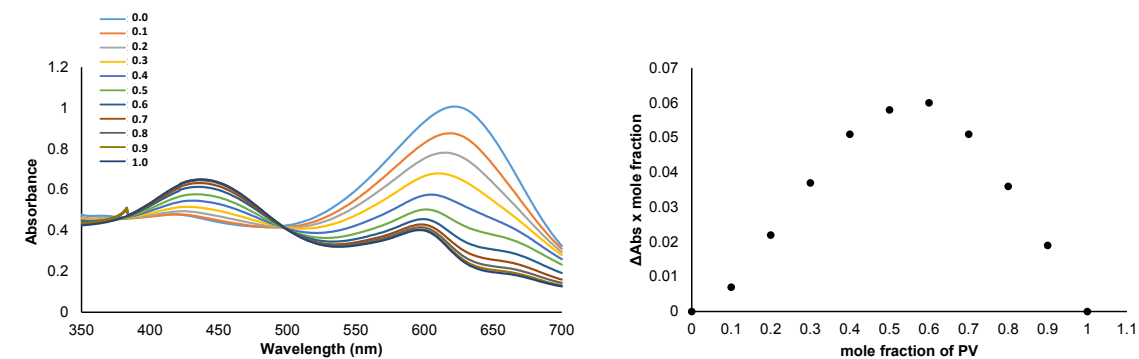
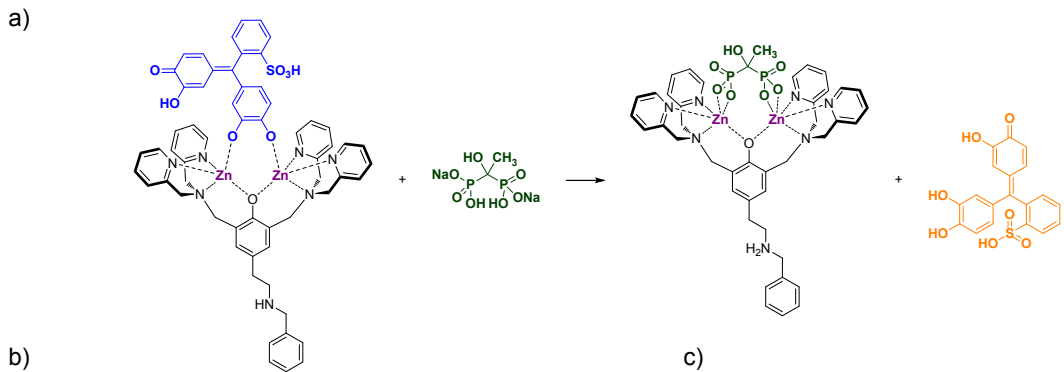


Figure S30: a) Indicator displacement assay between **2-PV** and etidronate b) UV spectra of 50 μ M **2-PV** titrated with increasing amounts of 1.25 mM etidronate in 10 mM HEPES solution, pH = 7.4. c) Job's plot of 50 μ M **2-PV** and etidronate in 10 mM HEPES solution at pH = 7.4.

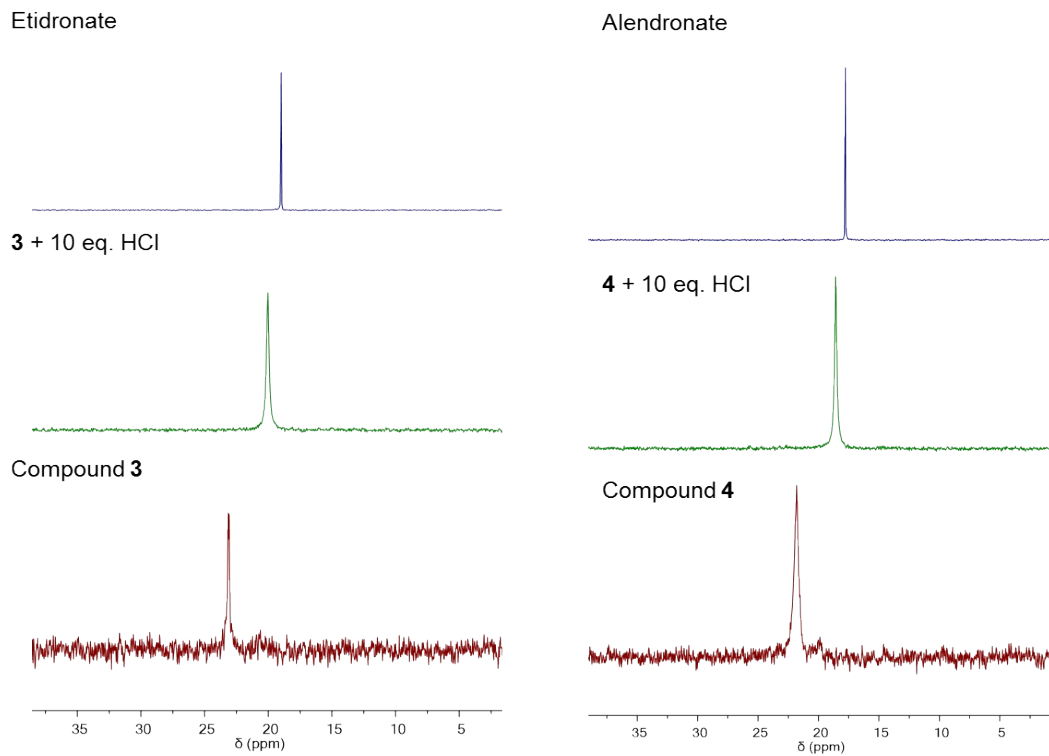


Figure S31: ^{31}P NMR spectra in D_2O of the compounds **3** and **4**, spectra after the addition of 10 eq. of HCl and spectra of the etidronate and alendronate.

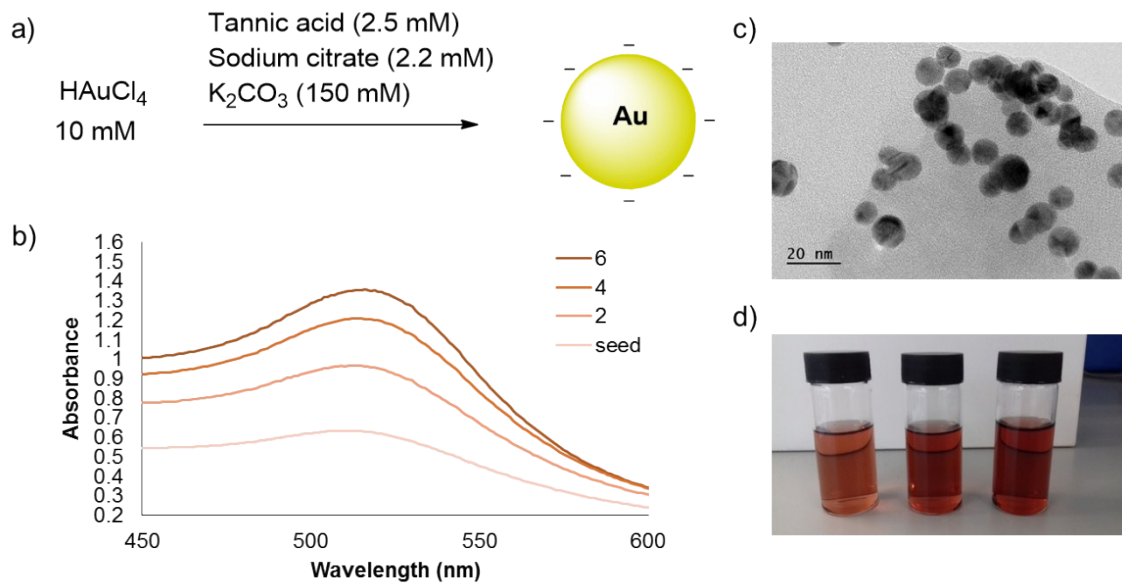


Figure S32: a) Synthesis of the gold nanoparticles; b) Changes in UV-Vis spectra as the size of the AuNPs grows; c) TEM images of the AuNPs; d) Changes in the coloration as the size of the AuNPs grows.

Table S1: Selected parameters for the unfunctionalised AuNPs obtained by UV-Vis spectroscopy.²

	λ_{max} (nm)	Abs (450 nm)	Conc. (nM)	NPs/mL
AuNPs	516	1.006	12.1	7.28×10^{12}

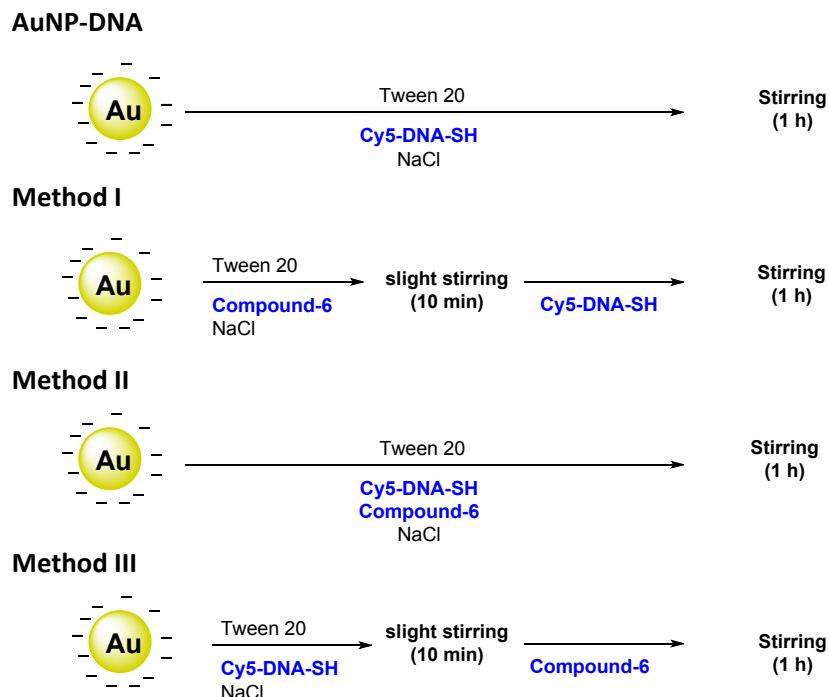


Figure S33: Optimization methods for loading the oligonucleotides strands and bimetallic zinc-complex on the AuNPs.

Table S2: Measured hydrodynamic diameters (d_h) and zeta potentials (ζ) for unfunctionalised AuNPs, AuNPs functionalised with DNA only and AuNPs functionalised with both DNA and di-zinc(II) receptor **6** (**AuNP-DNA-6**) synthesised *via* methods 1, 2 and 3.

	d_h (nm)	ζ (mV)
AuNPs	21.4 ± 0.2	-34.8 ± 1.2
AuNP-DNA	45.7 ± 0.4	-81.2 ± 0.9
Method 1	46.7 ± 0.7	-21.8 ± 0.9
Method 2	62.7 ± 0.9	-27.0 ± 0.4
Method 3	51.9 ± 1.7	-38.4 ± 1.7

Table S3: Measured values for the parameters: hydrodynamic diameters (d_h), and zeta potentials (ζ) of samples **AuNPs**, **AuNP-DNA**, **AuNP-DNA-5**, **AuNP-DNA-6** and **AuNP-DNA-7**.

	d_h (nm)	ζ (mV)
AuNPs	21.4 ± 0.2	-34.8 ± 1.2
AuNP-DNA	45.7 ± 0.4	-81.2 ± 0.9
AuNP-DNA-5	33.6 ± 0.5	-48.7 ± 2.2
AuNP-DNA-6	56.6 ± 2.0	-41.4 ± 1.5
AuNP-DNA-7	33.6 ± 0.5	-25.4 ± 1.6

Note: All samples were prepared using the same AuNPs solution with TEM diameter of 10.59 ± 1.8 nm.

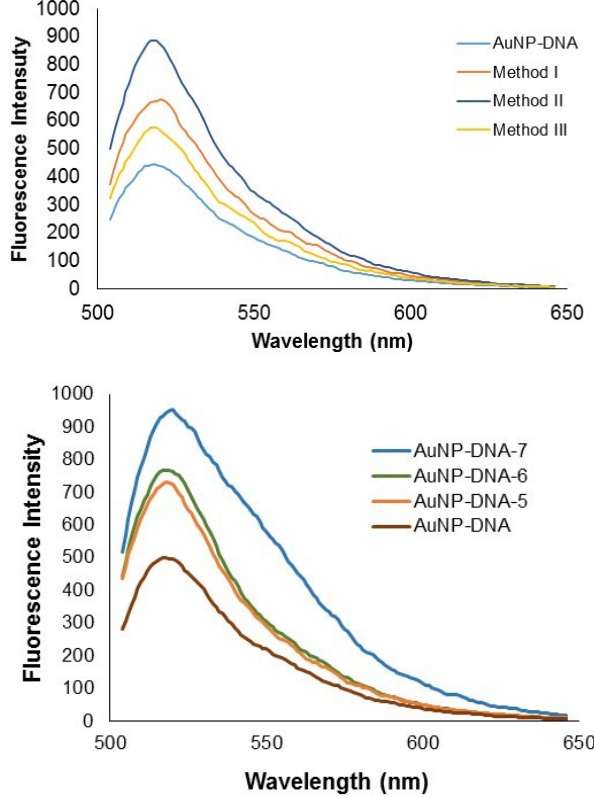


Figure S34: Fluorescence spectrums of the oligonucleotides from: (top) **AuNP-DNA** and **AuNP-DNA-6** prepared by methods I, II and III after exposure of the materials with mercaptoethanol (30 mM); (bottom) **AuNPs**, **AuNP-DNA**, **AuNP-DNA-5**, **AuNP-DNA-6** and **AuNP-DNA-7** after being treated with mercaptoethanol (30 mM).

References

- 1) A.L. Spek (2003, 2009) PLATON, A Multipurpose Crystallographic Tool, Utrecht University, Utrecht, The Netherlands. See also A.L. Spek, *Acta Cryst.*, 2015, **C71**, 9-18.
- 2) Haiss, W.; Thanh, N. T. K.; Aveyard, J.; Fernig, D. G. *Anal. Chem.* **2007**, *79*, 4215–4221.